

# First-principles analysis of spin-disorder resistivity of Fe and Ni

A. L. Wysocki,<sup>1,\*</sup> R. F. Sabirianov,<sup>2</sup> M. van Schilfgaarde,<sup>3</sup> and K. D. Belashchenko<sup>1</sup>

<sup>1</sup>*Department of Physics and Astronomy and Nebraska Center for Materials and Nanoscience, University of Nebraska–Lincoln, Lincoln, Nebraska 68588, USA*

<sup>2</sup>*Department of Physics and Nebraska Center for Materials and Nanoscience, University of Nebraska–Omaha, Omaha, Nebraska 68182, USA*

<sup>3</sup>*Department of Chemical and Materials Engineering, Arizona State University, Tempe, Arizona 85287, USA*

(Dated: November 3, 2018)

Spin-disorder resistivity of Fe and Ni and its temperature dependence are analyzed using non-collinear density functional calculations within the supercell method. Different models of thermal spin disorder are considered, including the mean-field approximation and the nearest-neighbor Heisenberg model. Spin-disorder resistivity is found to depend weakly on magnetic short-range order. If the local moments are kept frozen at their zero-temperature values, very good agreement with experiment is obtained for Fe, but for Ni the resistivity at elevated temperatures is significantly overestimated. Agreement with experiment for Fe is improved if the local moments are iterated to self-consistency. The overestimation of the resistivity for paramagnetic Ni is attributed to the reduction of the local moments down to  $0.35\mu_B$ . Overall, the results suggest that low-energy spin fluctuations in Fe and Ni are better viewed as classical rotations of local moments rather than quantized spin fluctuations that would require an  $(S + 1)/S$  correction.

## I. INTRODUCTION

Electron scattering off of spin fluctuations in magnetic metals results in an “anomalous” contribution to electric resistivity.<sup>1,2,3</sup> The analysis of this spin-disorder resistivity (SDR) is of interest because it can provide material-specific information on the character of spin fluctuations which is not easily accessible by other means. Scattering on spin disorder is also an important factor degrading the performance of magnetoresistive nanostructures in spintronic devices.

The magnitude of the spin-disorder contribution to resistivity is comparable to the phonon contribution near and above the Curie temperature  $T_c$ .<sup>1</sup> (Magnetic scattering amplitudes have no small parameter unless the local moments are small.) It is usually assumed that SDR is constant well above  $T_c$ . In this region Matthiessen’s rule is valid, and the phonon contribution can be fitted to the Bloch-Grüneisen formula. The excess resistivity in the whole temperature range may be attributed to spin disorder,<sup>4</sup> although one may expect deviations from Matthiessen’s rule at low temperatures where transport is carried by weakly interacting spin channels.<sup>5</sup> In addition, it was argued that in some cases (such as Ni) spin disorder may change the character of states on the Fermi level and thereby appreciably change the phonon contribution itself.<sup>1,2</sup>

Many authors have studied SDR theoretically using the  $s$ - $d$  model Hamiltonian.<sup>6,7,8,9</sup> In this approach the  $3d$  shells in transition metals (or  $f$  shells in rare earth metallic magnets) are assumed to be localized at atomic sites and partially filled, forming magnetic moments  $\hat{\mathbf{S}}_i$  that are coupled to the current-carrying conduction electrons by exchange interaction  $H_{sd} = -J_{sd} \sum_i \hat{\mathbf{S}}_i \hat{\mathbf{s}}_i$ , where  $J_{sd}$  is the local  $s$ - $d$  exchange coupling constant and  $\hat{\mathbf{s}}_i$  the spin-density operator of the conduction electrons at site

*i*. Thermal fluctuations of the  $d$ -electron spins generate an inhomogeneous exchange potential; in the Born approximation the SDR is then determined by the conduction electron band structure and the spin-spin correlation functions of  $d$ -electron spins.<sup>9</sup> If the scattering is approximated as being elastic, only equal-time spin correlators have to be considered. Further, if the mean-field approximation (MFA) is used for  $3d$  spin statistics, the SDR behaves as  $\rho_{\text{mag}}(T) = \rho_0[1 - M^2(T)/S(S + 1)]$ , where  $M(T) = \langle \mathbf{S}(T) \rangle$  is the magnetization at temperature  $T$  and  $\rho_0 \propto J_{sd}^2 S(S + 1)$ .<sup>6</sup> Note that above  $T_c$  SDR is constant and equal to  $\rho_0$ . The shape of the Fermi surface of conduction electrons is immaterial to this prediction as long as the scattering is elastic.<sup>9</sup>

The effects of magnetic short-range order (MSRO) on SDR have also been investigated within the  $s$ - $d$  model.<sup>7,8,10,11,12,13,14,15</sup> This problem has attracted considerable attention in connection with a “bump” in the resistivity that is observed near  $T_c$  in some magnetic metals (although it is usually quite small).<sup>1</sup> The analysis of critical MSRO effects showed that a cusp may appear near  $T_c$  due to long-wave critical fluctuations,<sup>7</sup> although it should usually be strongly suppressed by finite mean-free path and cancellations due to Fermi surface integration.<sup>10</sup> It was also found that the effect of MSRO and even its sign are sensitive to such details of the model as the conduction band occupation and the form of the scattering (pseudo)potential.<sup>12,13,14</sup>

Although the  $s$ - $d$  model provided physical insight into the mechanism of SDR, it suffers from serious limitations. First, the distinction between localized and conduction electrons is not justified in transition metals where  $3d$  electrons are itinerant and form the Fermi surface. Even if the current is dominated by light  $s$ -like bands that can be distinguished from heavy  $d$ -like bands, the relaxation rate is dominated by interband ( $s$ - $d$ ) scattering.<sup>16</sup>

Second, at elevated temperatures the scattering potential generated by spin disorder is of the order of the exchange splitting, which is not small compared to the bandwidth. This invalidates the Born approximation which is usually made in model calculations. Third, the  $s$ - $d$  model does not properly take into account the change of electronic structure due to disorder.

The first-principles approach to SDR is free from all these limitations and can be used for quantitative calculations of SDR. This is of particular interest for the theory of itinerant magnets, because, as mentioned above, SDR depends on spin-spin correlation functions. Different theories of itinerant magnetism make conflicting predictions for such properties as the degree of MSRO, the mean-squared magnetic moment, and their temperature dependence;<sup>17,18,19,20,21</sup> these quantities are quite hard to measure directly. By calculating SDR for a particular model of spin fluctuations and comparing the results with experiment, one can attempt to validate or rule out different spin-fluctuation models.

Earlier we have calculated the temperature dependence of SDR in Fe and Ni using supercell calculations within the tight-binding linear muffin-tin orbital (TB-LMTO) method using the mean-field distribution for spin orientation statistics.<sup>22</sup> Good agreement with experiment was obtained for Fe, but for paramagnetic Ni the SDR was found to be significantly overestimated. In this paper we analyze the temperature dependence of SDR for Fe and Ni in greater detail and consider the effects of magnetic ordering, MSRO, and local moment reduction. We also study the importance of the basis set size and self-consistency of the atomic potentials.

## II. GENERAL APPROACH AND METHODS

Our approach is based on noncollinear density functional theory (DFT). All the valence electrons are treated on the same footing, while the scattering potentials are determined by the self-consistent electron charge and spin densities. We use the TB-LMTO method<sup>23</sup> which represents the electronic density of the crystal as a superposition of overlapping atomic spheres; the electronic density inside each sphere is spherically symmetric. This method is known to work very well in close-packed materials, and it allows us to introduce spin disorder in various ways. In this work we used the rigid spin approximation which assumes that the spin density in each atomic sphere remains collinear, while the spin densities of different atomic spheres become noncollinear at finite temperatures. In the simplest model the electron charge and spin densities in all atomic spheres are taken from the ground state and frozen, while the directions of the spin moments in different spheres are randomized with the angular distribution function taken from MFA at the given temperature. This model is expected to work reasonably well for Fe which has a fairly stable local moment.<sup>24</sup> In Section III we show that this is indeed the case; however,

for Ni the paramagnetic SDR calculated in this way is about twice too large. In order to explain this discrepancy, the dependence of SDR on the degree of MSRO and on the magnitude of the local moment is studied in Sections IV and V.

We use the supercell approach and calculate the areal conductance of a layer of spin-disordered metal FM(D) sandwiched between fully ordered semi-infinite leads FM(O) made of the same metal (see Fig. 1). The resistivity is then proportional to the slope of the inverse conductance as a function of the disordered layer thickness, once the Ohmic limit is reached. For the given thickness of the FM(D) layer, the conductance of the system was averaged over several disorder configurations (typically 15). The planar system is represented by a laterally periodic prism with an axis along the [001] crystallographic direction, and care is taken to make sure that the conductance scales as the cross-section of the prism. To calculate the conductance we use the principal-layer Green's function technique<sup>25,26</sup> and the Landauer-Büttiker formalism<sup>27</sup> in the implementation allowing for noncollinearity in the active region.<sup>28</sup> This technique was employed before to study the effects of substitutional disorder on transport in magnetic multilayers;<sup>29</sup> it is similar to the supercell Kubo-Greenwood method used to calculate the residual resistivity of binary alloys.<sup>30</sup>

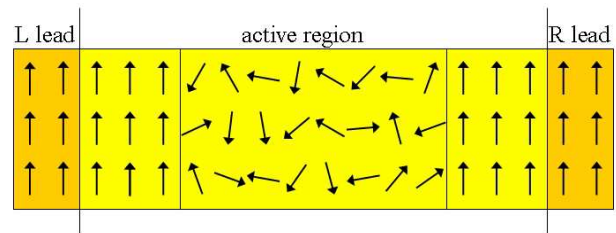


FIG. 1: (Color online) The schematic picture of the system used in the calculations. Vertical lines indicate the embedding planes.

If the atomic potentials in the supercell are not converged to self-consistency with the given spin disorder configuration, care needs to be taken to ensure local charge neutrality. Indeed, FM(D) and FM(O) materials have different Fermi levels that must normally be matched by the contact voltage. In order to enforce charge neutrality in the FM(D) region, a constant potential shift was introduced in this region so that the charge in the central part of FM(D) averaged over disorder realizations was zero. This potential shift plays the role of the contact voltage. Note that no matter how the FM(O)/FM(D) interfaces are treated (self-consistently or not), they add contact resistances to the circuit. However, since the *resistivity* of the FM(D) material is extracted from the thickness dependence of the resistance in the Ohmic limit, the simplified treatment of interfaces has no effect on the results.

### III. SPIN-DISORDER RESISTIVITY IN THE MEAN-FIELD APPROXIMATION

#### A. Paramagnetic state

In this section we analyze the temperature dependence of SDR for iron and nickel using MFA for thermal spin disorder; the spin-spin correlator is purely local in this approximation. First we consider the paramagnetic state where the angular distribution function is isotropic, and the resulting SDR is temperature-independent.

We need to make a physically reasonable choice of atomic potentials for the conductance calculations. It is known that the local moments in Fe are quite stable;<sup>17</sup> in particular, the DLM method, which employs the coherent potential approximation for spin-disordered states, shows only a small reduction of the local moment in paramagnetic Fe compared to its ground-state value.<sup>24</sup> As seen below, direct averaging of self-consistent local moments in the paramagnetic states gives a similar result. Therefore, for Fe it is reasonable to use frozen atomic potentials taken from the zero-temperature ground state in all calculations. We have also checked the effect of self-consistency on SDR in Fe and found it to be small (see below). The situation is entirely different for Ni, where the local moment depends on the magnetic state; in particular, it vanishes altogether in the paramagnetic DLM approximation.<sup>34</sup> Since longitudinal spin fluctuations (that are absent in our approach) can at least partially restore the local moments,<sup>17</sup> it is not *a priori* clear how the atomic potentials should be modified for Ni. In this section we use frozen atomic potentials; the necessary corrections are discussed later.

Fig. 2 shows the inverse areal conductance for paramagnetic Fe and Ni as a function of the disordered FM(D) region thickness. Here we used the frozen ground-state atomic potentials and the LMTO basis including  $s$ ,  $p$ , and  $d$  orbitals ( $l_{max} = 2$ ). The supercell cross-sections contained  $4 \times 4$  (for Fe) and  $3 \times 3$  (for Ni) cubic unit cells with edges oriented along the  $[100]$  directions. Almost perfect Ohmic behavior is apparent for both Fe and Ni, which establishes the validity of our approach.

Table I lists the values of SDR found for paramagnetic Fe and Ni using different supercell cross-sections, LMTO bases truncated at  $l_{max} = 2$  and  $l_{max} = 3$  (the latter includes  $f$  orbitals), as well as the value found using self-consistent (rather than frozen) atomic potentials for Fe. It is seen that the results are well converged with respect to the supercell cross-section, and even  $2 \times 2$  supercells provide sufficient accuracy. This is reasonable because the mean-free path in the paramagnetic state is small.

The calculations with self-consistent atomic potentials were performed as follows. In order to reduce the statistical error, the averaging of the conductance was performed using the same sets of random spin disorder configurations as in the calculation with frozen potentials. For each individual spin configuration the atomic potentials were iterated to self-consistency using the Fermi distri-

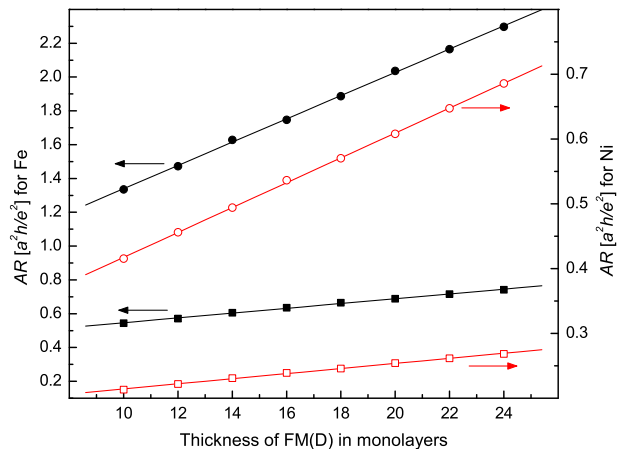


FIG. 2: (Color online) The area-resistance product  $AR$  of the FM(O)/FM(D)/FM(O) systems as a function of the FM(D) layer thickness for bcc Fe (black filled symbols) and fcc Ni (red or gray empty symbols) obtained with  $l_{max} = 2$ . Circles and squares correspond, respectively, to the paramagnetic state and to the lowest temperature for which the calculations were made.  $4 \times 4$  and  $3 \times 3$  supercells were used for Fe and Ni, respectively, with edges along the  $[100]$  directions. Straight lines show the linear fitting; error bars are smaller than the size of the symbols.

TABLE I: Spin-disorder resistivity in  $\mu\Omega\text{-cm}$  for paramagnetic bcc Fe and fcc Ni. The calculated values are given for basis sets with  $l_{max} = 2$  and 3, as well as for different lateral cell sizes with edges along the  $[100]$  directions. SC denotes calculations with self-consistent potentials. Standard deviations of SDR due to limited disorder sampling are included.

Metal and basis	$M, \mu_B$	$2 \times 2$	$3 \times 3$	$4 \times 4$	Exp. <sup>4</sup>
Fe: $l_{max} = 2$	2.29	$106 \pm 1.8$	$101 \pm 1.3$	$102 \pm 1.0$	80
$l_{max} = 3$	2.22	$86 \pm 1.6$	$87 \pm 7.1$	$85 \pm 7.4$	80
$l_{max} = 2$ , SC	2.21	$88 \pm 3.7$			80
Ni: $l_{max} = 2$	0.66	$34 \pm 0.6$	$35 \pm 0.4$		15
$l_{max} = 3$	0.63	$29 \pm 0.6$			15

bution function corresponding to the experimental  $T_c$  of Fe. The resulting distribution of the sites over the magnitude of the local magnetic moment is shown in Fig. 3; this distribution is Gaussian with a rather small width. The average local moment is only reduced by 3-4% from its ground state value. This small reduction appears to be similar to the DLM calculations of Ref. 20, while Ref. 24 obtained a somewhat larger reduction. The self-consistent density of states (not shown) is very similar to the one generated by the frozen ground-state atomic potentials (see Fig. 4e below).

The addition of  $f$  orbitals to the LMTO basis reduces the calculated SDR by approximately 15% for both Fe and Ni. Self-consistency in the paramagnetic state of Fe results in a similar reduction. This similarity suggests that the main reason for this SDR decrease is the reduc-

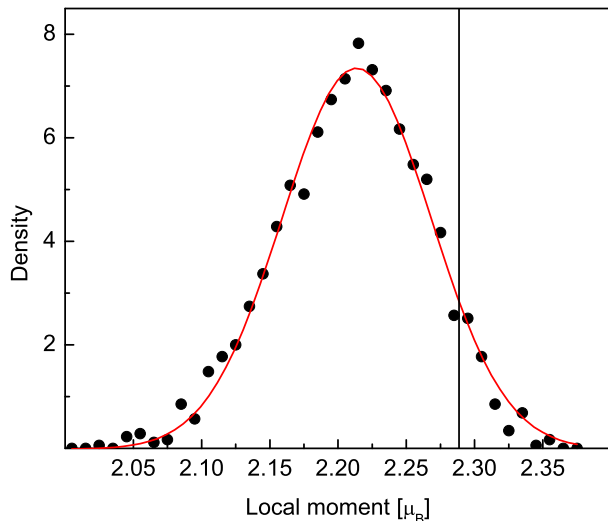


FIG. 3: (Color online) Distribution of the local magnetic moment in self-consistent fully spin-disordered bcc Fe. The Fermi temperature is equal to the experimental  $T_c$ . The vertical line shows the local moment at  $T = 0$ . The red (solid) curve shows the Gaussian fit to the data.

tion of the local moment, which is, incidentally, very similar in both cases. In order to check this, we performed additional calculations for Fe in which the  $f$  channel was added to the basis while the charge density was kept unchanged from the self-consistent one with  $l_{max} = 2$ . For the frozen potential case, SDR reduced slightly from 106 to 100  $\mu\Omega\cdot\text{cm}$ ; for the self-consistent paramagnetic case, it only reduced from 88 to 86  $\mu\Omega\cdot\text{cm}$ , which is within the error bar. Thus, the effect of  $l_{max}$  *per se* on SDR is very small for Fe. This is somewhat different from the binary alloy systems considered by other authors using both TB-LMTO and KKR (Korringa-Kohn-Rostocker) methods, where a larger effect of adding  $f$  states was found.<sup>31,32</sup> In view of the weak dependence of SDR on  $l_{max}$ , below we use  $l_{max} = 2$  in all calculations for  $T < T_c$ .

The experimental estimates of SDR in the paramagnetic state<sup>4</sup> are listed in the last column of Table I. The agreement with experiment for Fe is quite satisfactory, and it is in fact improved if the reduction of the local moment is included. In Ni the SDR calculated with frozen atomic potentials is overestimated by a factor of 2. This is not surprising, because, as mentioned above, the use of frozen atomic potentials is not justified for Ni. In order to understand the origins of the disagreement with experiment for Ni, possible modifications of the statistical model for the paramagnetic state must be considered; this is done below in Sections IV and V.

Recently, Buruzs *et al.*<sup>33</sup> calculated the SDR for Fe and Co using the disordered local moment (DLM) approach within the Korringa-Kohn-Rostocker method and found that their method significantly overestimates the paramagnetic SDR in these metals. The source of disagreement with our supercell method for Fe is unknown to us.

## B. Temperature dependence in the ferromagnetic state

In this section we consider ferromagnetic state of Fe and Ni. We use frozen ground-state potentials and the basis with  $l_{max} = 2$ . As mentioned above, this approximation is reasonable for Fe, while for Ni it is not applicable at high temperatures; nevertheless, comparison of these two systems will allow us to draw important conclusions. For the ferromagnetic state the spin configurations were generated using the mean-field distribution function

$$p(\theta) \propto e^{-\mathbf{H}_{\text{eff}} \cdot \boldsymbol{\mu}/T}, \quad H_{\text{eff}}(T) = \frac{3M(T)T_c}{\mu M(0)} \quad (1)$$

where  $\theta$  is the angle between the local moment  $\boldsymbol{\mu}$  and the magnetization axis,  $M(T)$  is the magnetization at temperature  $T$  in MFA, and  $\mathbf{H}_{\text{eff}}$  is the Weiss field. This distribution function depends only on  $T/T_c$ .

Before we turn to the temperature dependence of SDR, let us look at the electronic structure of Fe and Ni with spin disorder. The spin-resolved DOS of Fe and Ni is shown in Figs. 4 and 5 for several temperatures. These data were obtained by projecting the site-resolved DOS onto local spin-up and spin-down states (in the local reference frame where the  $z$  axis is parallel to the local moment) and subsequent averaging over bulk-like sites and spin disorder configurations generated according to Eq. (1). The paramagnetic DOS of Fe is very similar to the KKR-DLM results.<sup>24</sup> As the temperature is increased from 0 to  $T_c$ , the spin-up and spin-down states randomly hybridize with each other, the peaks broaden, and the van Hove singularities are washed out. The mean-squared deviation of the DOS from its average (shown by dashed lines) is quite small, which is a direct consequence of the large coordination number. In Fe the spin splitting is almost independent on temperature, while in Ni it is much reduced as  $T$  gets close to  $T_c$ . Note that the frozen atomic potentials in Ni are very far from self-consistency at elevated temperatures, but a self-consistent treatment neglecting longitudinal spin fluctuations would be meaningless. We will return to this issue in Section V.

Let us now discuss the temperature dependence of SDR. While we found above that  $2 \times 2$  supercells were sufficiently large for the paramagnetic state, additional care needs to be taken at lower temperatures where the mean-free path becomes longer. We found that  $4 \times 4$  supercells for Fe and  $3 \times 3$  for Ni demonstrate linear dependence of the conductance on the length of the supercell for all temperatures down to about  $T_c/3$  (see Fig. 2). This behavior agrees with a simple mean-free path estimate using the free-electron formula  $l = \frac{3}{4}AR_{\text{bal}}/\rho$ , where  $AR_{\text{bal}}$  is the ballistic area-resistance product;  $l$  does not exceed the lateral cell size in this temperature range. Another indication of the Ohmic behavior comes from the distribution of the current over the spin channels. The conductance of the FM(O)/FM(D)/FM(O) system is a sum of four partial conductances,  $G_{\uparrow\uparrow}$ ,  $G_{\downarrow\downarrow}$ ,  $G_{\uparrow\downarrow}$ ,  $G_{\downarrow\uparrow}$  (the latter

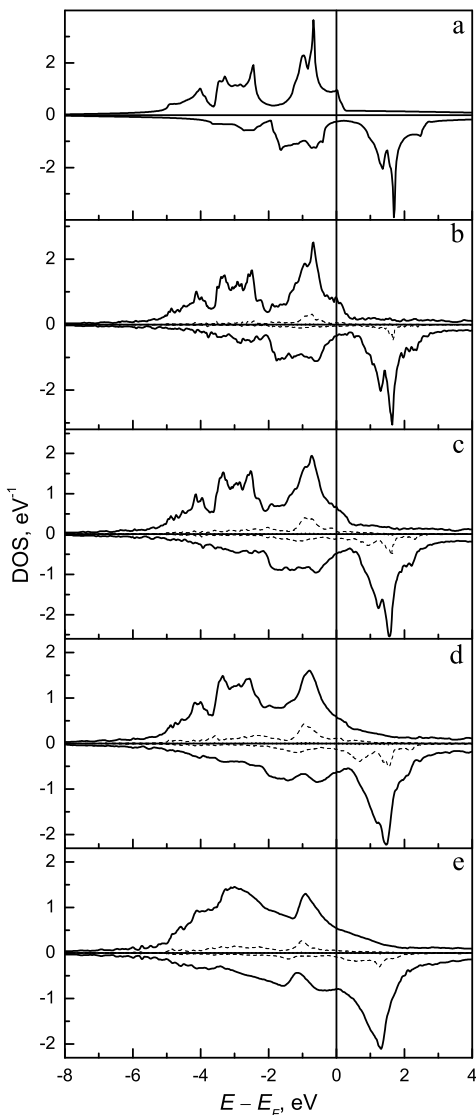


FIG. 4: Spin-resolved density of states (solid lines) for bcc Fe averaged over random spin configurations with the mean-field distribution function (1); (a)  $T = 0$ , (b)  $T = 0.25T_c$ , (c)  $T = 0.5T_c$ , (d)  $T = 0.75T_c$ , and (e)  $T = T_c$ . Dashed lines show the mean-square deviation of the DOS on a given site from its ensemble average.

two are equal). Spin-conserving and spin-flip scattering have similar rates in our spin-disorder problem (as long as the temperature is not too low), and therefore the electrons “forget” their spin over their mean-free path. Therefore, in the Ohmic limit the partial conductances must be proportional to the number of channels in the left and right leads for the corresponding spin channels:  $G_{\sigma\sigma'} \propto M_{\sigma}^L M_{\sigma'}^R$ . This implies that in this regime we should have  $G_{\uparrow\uparrow} G_{\downarrow\downarrow} = G_{\uparrow\downarrow} G_{\downarrow\uparrow}$ . This relation does indeed hold down to  $T \sim T_c/3$  unless the thicknesses of the FM(D) region is very small.

The dependence of the calculated SDR for Fe and Ni

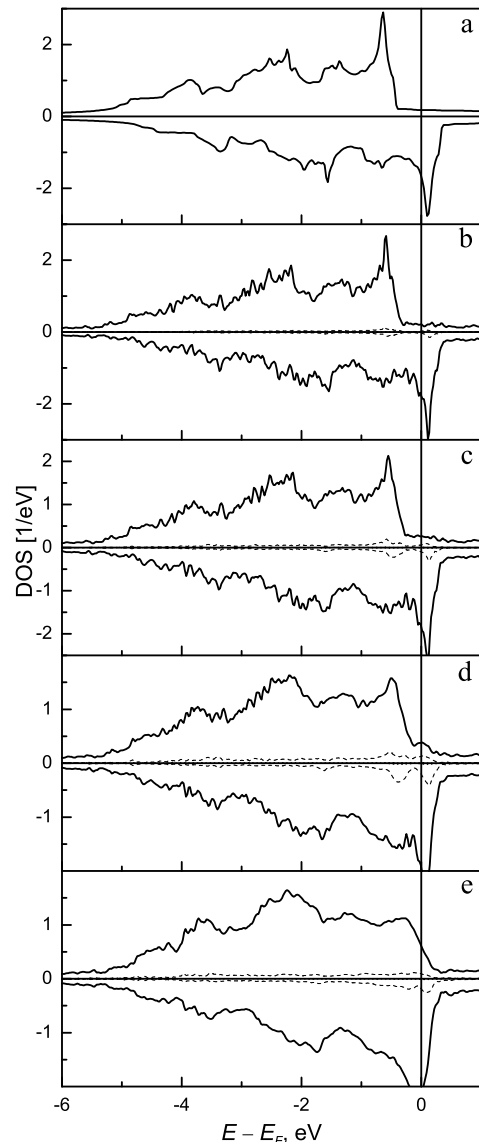


FIG. 5: Same as in Fig. 4 but for fcc Ni.

on the magnetization is plotted in Fig. 6 along with the experimental data<sup>4</sup> (those for  $M(T)$  were taken from Ref. 37). The results for Fe agree rather well with experiment, especially at lower temperatures where the magnetic excitations are dominated by spin waves and our classical approach is, strictly speaking, invalid. This surprising finding is due to the fact that SDR in Fig. 6 is plotted as a function of the long-range order parameter and that, as we show below in Section IV, the SDR in Fe is insensitive to MSRO. The calculated SDR exhibits linear dependence on  $M^2(T)$  up to  $T_c$ , while the experimental data deviate downward from the straight line. This deviation may be attributed to a small reduction of the local moment at elevated temperatures, as discussed in the previous section.

For Ni the deep low-temperature region could not be

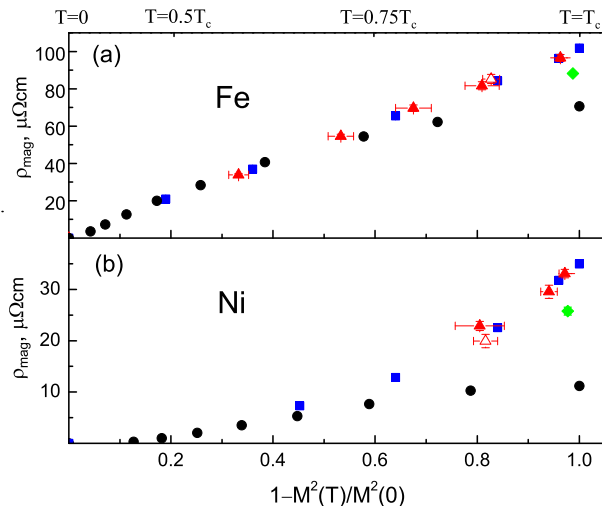


FIG. 6: (Color online) Dependence of spin-disorder resistivity on the magnetization for (a) Fe, and (b) Ni. Black circles denote experimental data combining Ref. 4 for  $\rho_{\text{mag}}(T)$  and Ref. 37 for  $M(T)$ . Blue (black) squares show mean-field calculations, filled red (gray) triangles denote Monte Carlo results, and green (gray) diamonds show reverse Monte Carlo calculations. The empty red (gray) triangles show Monte Carlo results with larger cells:  $6 \times 6$  for Fe and  $4 \times 4$  for Ni. The upper axis shows temperatures corresponding to the given magnetization in MFA. The error bars along the  $x$  and  $y$  axes show statistical uncertainties where they exceed the size of the symbols. All results are for  $l_{\text{max}} = 2$ .

accessed due to the increased mean-free path. Still, the agreement with experiment at lower temperatures is good, while at higher temperatures the calculated SDR strongly deviates upwards from experimental data. This deviation indicates the inadequacy of our spin fluctuation model; its possible modifications are studied in the following sections.

The qualitative features of the *calculated* temperature dependence of SDR (with frozen atomic potentials) are different for Fe and Ni. It is seen in Fig. 6 that for Fe the SDR is proportional to  $1 - M^2(T)/M^2(0)$  in agreement with the predictions of the *s-d* model if spin fluctuations are treated classically. On the other hand, for Ni this relation does not hold. As mentioned in the Introduction, the change of electronic structure due to spin disorder may lead to deviations from *s-d* model predictions.

As seen in Figs. 4 and 5, the densities of states change quite appreciably with temperature for both Fe and Ni. Therefore, it may seem surprising that for Fe the temperature dependence of SDR agrees with the *s-d* model. Still, one can understand the difference between Fe and Ni using the following considerations. First, as seen in Fig. 5, the exchange splitting in Ni is strongly reduced at elevated temperatures, which results in the lifting of the heavy majority-spin *3d* bands up to the Fermi level. Scattering into these final states from the light bands becomes possible, which decreases the lifetime of the lat-

ter. This mechanism was invoked by Mott<sup>2</sup> to argue that the reduction of the spin splitting in Ni can result in an anomalous temperature dependence of the *phonon* resistivity. The same argument applies to SDR considered here. According to Fig. 5, this happens approximately at  $T = 0.75T_c$ , which roughly corresponds to the upturn of SDR seen in Fig. 6b. On the other hand, for Fe, as seen in Fig. 4, the exchange splitting is constant and no new bands appear at the Fermi level. Consequently, no additional temperature dependence is introduced and SDR scales as  $1 - M^2(T)/M^2(0)$ .

While plausible, the above arguments are not conclusive, because they assume without proof that the scattering matrix elements between the light and heavy bands are large. On a more subtle level, one may speculate that the difference between Fe and Ni can be understood based on the relation between disorder broadening and spin splitting. At the given wavevector, the spectral function consists of delta-function peaks corresponding to majority and minority-spin states. In the presence of spin disorder, the spin states on neighboring sites are allowed to hybridize with random matrix elements, and the delta-function peaks broaden. At low temperature the broadening is small, and the peaks corresponding to different spins are well separated in energy from each other. However, at higher temperatures some of these peaks can merge and form common, “virtual-crystal-like” bands. Calculations of the paramagnetic spectral functions using the DLM method indicate that in Fe the majority and minority-spin states remain separated through large portions of the Fermi surface even above  $T_c$ .<sup>35</sup> On the other hand, in Ni the majority and minority-spin states are mixed in the paramagnetic state.<sup>35</sup> Therefore, at certain temperature below  $T_c$  there is a crossover from separated to mixed-spin bands. The lifetime is expected to decrease as the bands merge, which again explains the upturn of SDR from the straight line in Fig. 6b.

#### IV. EFFECT OF MAGNETIC SHORT-RANGE ORDER

As mentioned above, short-range order can sometimes have a significant effect on resistivity. In this section we analyze the effect of MSRO on SDR in Fe and Ni. In particular, it is important to check whether the large disagreement with experiment for Ni found in Section III can be due to the use of MFA which neglects MSRO. This is especially interesting because strong MSRO in Ni has been suggested by some experiments<sup>17,36</sup> and theories.<sup>18,19</sup>

Spin disorder configurations with MSRO were generated using the Monte Carlo (MC) method for the classical Heisenberg model with nearest-neighbor (NN) exchange interaction on bcc and fcc lattices (for Fe and Ni, respectively). These configurations were used to calculate SDR as described above, which can then be compared with MFA results. As before, we usually used  $4 \times 4$  and

TABLE II: Spin-spin correlators  $C_{0i}$  for the first three shells of nearest neighbors ( $i = 1, 2, 3$ ) and the local correlator ( $i = 0$ ) are shown for Fe and Ni for each considered temperature in Monte Carlo simulations and for reverse Monte Carlo method. The values of the correlators were found using  $4 \times 4$  cells and averaging over the lengths that were used in transport calculations. The Curie temperature for bcc and fcc nearest-neighbor Heisenberg model was obtained using the fourth order cumulant method. The values of SDR are compared with MFA results corresponding to the same  $M^2$ . The listed uncertainties are due to the limited disorder sampling.

Metal, cross-section	$T/T_c$	$C_{0i} = \langle \mathbf{e}_0 \mathbf{e}_i \rangle - \langle \mathbf{e}_0 \rangle \langle \mathbf{e}_i \rangle$				$\rho_{\text{mag}}, \mu\Omega \cdot \text{cm}$	
		$i = 0$	$i = 1$	$i = 2$	$i = 3$	MC or RMC	MFA
Fe, $4 \times 4$	$\infty$	1	0	0	0	$101.9 \pm 1.0$	$101.9 \pm 1.0$
Fe, $4 \times 4$	1.22	$0.96 \pm 0.01$	$0.15 \pm 0.01$	$0.07 \pm 0.01$	$0.04 \pm 0.01$	$96.6 \pm 1.9$	$97.6 \pm 0.5$
Fe, $4 \times 4$	0.98	$0.81 \pm 0.03$	$0.14 \pm 0.03$	$0.08 \pm 0.03$	$0.04 \pm 0.03$	$81.6 \pm 2.1$	$82.4 \pm 0.4$
Fe, $6 \times 6$	0.98	$0.83 \pm 0.02$	$0.16 \pm 0.02$	$0.09 \pm 0.02$	$0.06 \pm 0.02$	$81.4 \pm 2.3$	$84.4 \pm 0.4$
Fe, $4 \times 4$	0.85	$0.68 \pm 0.04$	$0.14 \pm 0.04$	$0.09 \pm 0.04$	$0.07 \pm 0.04$	$69.6 \pm 1.8$	$69.1 \pm 0.4$
Fe, $4 \times 4$	0.73	$0.53 \pm 0.03$	$0.09 \pm 0.03$	$0.05 \pm 0.03$	$0.03 \pm 0.03$	$54.6 \pm 1.8$	$53.9 \pm 0.3$
Fe, $4 \times 4$	0.49	$0.33 \pm 0.02$	$0.06 \pm 0.02$	$0.04 \pm 0.02$	$0.02 \pm 0.02$	$33.8 \pm 0.7$	$33.6 \pm 0.2$
Fe, $4 \times 4$	RMC	$0.99 \pm 0.01$	$0.30 \pm 0.01$	$0.16 \pm 0.01$	$0.05 \pm 0.01$	$88.2 \pm 1.3$	$100.7 \pm 0.5$
Ni, $3 \times 3$	$\infty$	1	0	0	0	$34.9 \pm 0.4$	$34.9 \pm 0.4$
Ni, $3 \times 3$	1.27	$0.97 \pm 0.01$	$0.12 \pm 0.01$	$0.04 \pm 0.01$	$0.02 \pm 0.01$	$33.1 \pm 0.8$	$32.4 \pm 0.3$
Ni, $3 \times 3$	1.11	$0.94 \pm 0.02$	$0.15 \pm 0.02$	$0.07 \pm 0.02$	$0.04 \pm 0.02$	$29.5 \pm 1.3$	$30.0 \pm 0.4$
Ni, $3 \times 3$	0.95	$0.80 \pm 0.05$	$0.14 \pm 0.05$	$0.08 \pm 0.05$	$0.06 \pm 0.05$	$22.9 \pm 0.9$	$20.4 \pm 0.7$
Ni, $4 \times 4$	0.95	$0.82 \pm 0.02$	$0.15 \pm 0.03$	$0.08 \pm 0.03$	$0.06 \pm 0.03$	$19.9 \pm 1.3$	$21.6 \pm 0.7$
Ni, $4 \times 4$	RMC	$0.98 \pm 0.01$	$0.31 \pm 0.01$	$0.12 \pm 0.01$	$0.09 \pm 0.01$	$25.8 \pm 0.8$	$33.2 \pm 0.3$

$3 \times 3$  supercells for Fe and Ni, respectively, which was sufficient to achieve Ohmic scaling of the conductance.

The results of SDR calculations for this model are shown in Fig. 6. The MC results for SDR are very close to MFA results corresponding to the same magnetization, in spite of the presence of MSRO in the MC model. We also performed additional calculations with larger cell cross-sections ( $6 \times 6$  for Fe and  $4 \times 4$  for Ni) in order to check whether the finite-size effects are important close to  $T_c$ . The results are shown by empty and full inverted triangles in Fig. 6; the temperature was taken to be the same as for the neighboring point for a smaller cross-section. It is clear that finite-size effects have no appreciable effect on SDR. Thus, it appears that the spin-spin correlations on the length scales comparable to our supercell lateral dimension have negligible effect on SDR, in agreement with the conclusions of Ref. 10.

These results clearly show that MSRO characteristic for the NN Heisenberg model has virtually no effect on SDR in Fe and Ni. The magnitude of MSRO is illustrated in Table II where the spin-spin correlators for the first three shells of nearest neighbors are shown together with the corresponding resistivities. While MSRO in the NN Heisenberg model for the close-packed lattices considered here is not strong, it is seen that its effect on SDR is much smaller even compared with the values of the NN spin-spin correlators. This insensitivity is likely due to the averaging over all the electronic states on the Fermi surface,<sup>10</sup> which should be very effective in destroying the interference from scattering at different sites in transition metals with complicated Fermi surfaces. In fact,

this averaging is also responsible for the small standard deviation of the local DOS from its mean (Fig. 4) and justifies the DLM approach for transition metals.

The spin-spin correlation function in real materials may be more complicated than in the NN Heisenberg model. However, if the interaction has a longer range while remaining mainly ferromagnetic, the MSRO must be *weaker* compared to the NN model.<sup>38</sup> First-principles calculations for both ferromagnetic and paramagnetic nickel show that the exchange parameters beyond nearest neighbors, while being much smaller than the dominant NN exchange, stay mainly ferromagnetic.<sup>20,39</sup> Interaction of this kind can not support stronger MSRO compared to the NN Heisenberg model.

Since the complete insensitivity of the resistivity to MSRO within the NN Heisenberg model is somewhat surprising, we have checked whether it is possible to observe some change of SDR using spin configurations with an artificially introduced stronger MSRO. For this purpose we used the reverse Monte Carlo (RMC) method<sup>40</sup> to produce a set of spin configurations with almost zero magnetization and deliberately targeting strong MSRO in the NN shell. Due to geometrical constraints, the spin-spin correlators in different neighbor shells are not independent. We found it quite difficult to produce strongly correlated nearest neighbors and at the same time avoid unphysical artefacts in the long-range behavior of the correlation function. The spin-spin correlators for the first three shells of neighbors in our RMC model are listed in Table II. The corresponding values of SDR calculated for Fe and Ni with this set of spin configurations are also

listed in Table II and shown by full and empty diamonds in Fig. 6. Here we used  $4 \times 4$  supercells for both Fe and Ni and checked for finite-size effects using  $6 \times 6$  supercells for Fe (essentially no difference was observed compared to  $4 \times 4$  cells). As seen in Table II, the MSRO in this model is significantly stronger compared to the NN Heisenberg model. The effect of this strong MSRO on the calculated SDR is now noticeable but still relatively small; the SDR is reduced compared to its MFA values by 12% for Fe and 22% for Ni.

## V. EFFECT OF THE LOCAL MOMENT REDUCTION

Reduction of the local moment is a universal feature of itinerant magnets as revealed by spin fluctuations theories.<sup>17</sup> As discussed in Section III, the local moment in Fe is very stable and changes only slightly in the paramagnetic state compared to zero temperature. Therefore, our calculations based on the ground-state value of the local moment agree well with experiment for Fe. Still, the SDR is sensitive to the local moment, and a small reduction of it noticeably improved the agreement with experiment at higher temperatures. Since the SDR was found to be insensitive to MSRO, it is reasonable to attribute the large overestimation of the high-temperature SDR in Ni to the neglect of the local moment reduction. Here we study this issue in detail.

In the paramagnetic DLM state the local moment in Ni vanishes,<sup>34</sup> but it is partially restored by longitudinal spin fluctuations.<sup>17,20</sup> Following the idea of separation of low and high-energy fluctuations, we assume that the current-carrying quasiparticles near the Fermi level experience the averaged exchange-correlation field generated by fast longitudinal spin fluctuations, and that this “mean field” is adequately represented by noncollinear DFT with disordered local moments constrained to their square-averaged values. The atomic potentials are therefore obtained using the fixed spin method<sup>41</sup> with the value of the constrained local moment treated as an adjustable parameter, which has a physical meaning and can be measured experimentally. Other approximations are, in principle, possible; for example, the longitudinal spin fluctuations can be explicitly included in the same noncollinear DFT approach, i. e. they can be considered to be “slow” rather than “fast.” Since the separation in slow and fast degrees of freedom is not well defined, we did not attempt to study the role of these additional fluctuations.

The calculated paramagnetic SDR of Ni as a function of the local moment is shown in Table III. As seen, SDR is very sensitive to the value of the local moment. Comparison with experimental SDR shows that our predicted value of the square-averaged local moment in paramagnetic state of Ni is equal to  $0.35\mu_B$  (using the more accurate basis set with  $l_{max} = 3$ ). Unfortunately, we are not aware of experimental measurements suitable for com-

TABLE III: Spin-disorder resistivity in  $\mu\Omega\text{-cm}$  for paramagnetic Ni as a function of the fixed local moment.  $2 \times 2$  supercells and basis sets with  $l_{max} = 2$  and  $l_{max} = 3$  were used. Standard deviations of SDR due to limited disorder sampling are included.

Local moment, $\mu_B$	0.66	0.5	0.4	0.3	Exp. <sup>4</sup>
$l_{max} = 2$	$34 \pm 0.6$	$27 \pm 0.5$	$21 \pm 0.4$		15
$l_{max} = 3$	$29 \pm 0.6^a$	$23 \pm 0.5$	$18 \pm 0.4$	$12 \pm 0.3$	15

<sup>a</sup>This value corresponds to unconstrained local moment of  $0.63\mu_B$ .

parison with this prediction.

## VI. DISCUSSION AND CONCLUSIONS

Numerous previous studies<sup>6,7,8,9,10</sup> based on the  $s$ - $d$  model concluded that SDR in the paramagnetic state is essentially proportional to  $J_{sd}^2 S(S+1)$  where  $S$  is the spin of the partially filled  $3d$  shell. This dependence is easy to understand based on the Fermi golden rule with averaging over the initial states of the  $3d$  spin. In our treatment based on noncollinear DFT, the exchange-correlation field with randomized directions on different sites plays the role of the  $s$ - $d$  Hamiltonian. However, contrary to the  $s$ - $d$  model, the  $3d$  spin is treated classically, i. e.  $\mathbf{S}$  is just a classical vector and not an operator. The Fermi golden rule in our case would give a paramagnetic SDR proportional to  $J_{sd}^2 S^2$ . Thus, if the  $S(S+1)$  factor were correct, noncollinear DFT calculations would underestimate the paramagnetic SDR by a factor  $(S+1)/S$ . This factor is close to 2 for Fe and more than 3 for Ni. In reality, the calculated SDR agrees well with experiment for Fe and is *overestimated* for Ni (if the local moment reduction is not included). We believe that these results provide clear evidence against the  $S(S+1)$  factor which appears if the local moments are treated as local atomic spins. Instead, the classical description of the local magnetic fluctuations in the spirit of the DLM approach is supported by our results. We suggest that the itinerancy of the  $3d$  electrons is crucial for this behavior. Qualitatively, one can argue that the low-energy fluctuations in Fe or Ni on the scale of  $kT$  (which the resistivity is most sensitive to) are similar to classical rotations of the local moments rather than quantum fluctuations of localized spins. It would be interesting to investigate this issue for magnets with a varying degree of localization, including rare-earth systems.

Some poorly controlled assumptions are involved in the extraction of  $\rho_{mag}$  from the experimental data.<sup>4</sup> First, it is assumed that  $\rho_{mag}$  is constant in the wide temperature range above  $T_c$  where the total resistivity is linear in  $T$ . This assumption implies that the local moments (or at least their mean-squared average) are constant in this range. Spin fluctuation theories for itinerant metals show that the local moments may change with temperature above  $T_c$ .<sup>17,20,21</sup> Such change will contribute to the slope

of  $\rho$  above  $T_c$ , and hence the separation of  $\rho_{\text{mag}}$  from the phonon contribution would be inaccurate.

On the other hand, it has been argued that the phonon contribution to the resistivity may be sensitive to spin disorder, because the latter may change the character of states at the Fermi level.<sup>1,2</sup> In particular, in Ni the filled majority-spin  $d$  states may be lifted up to the Fermi level by spin disorder, thereby facilitating interband  $s$ - $d$  scattering by phonons. This effect may therefore introduce an unusual temperature dependence of the phonon contribution, which makes spin disorder and phonon effects non-additive, even if the scattering rates themselves obey Matthiessen's rule. Since we have not studied this effect here, our comparison of SDR with experiment for Ni is incomplete. However, the phonon contribution can be expected to follow the Bloch-Grüneisen form above  $T_c$  with the electron-phonon scattering renormalized by spin disorder; therefore, the influence of spin disorder on the phonon contribution should not invalidate the procedure used for subtracting this contribution above  $T_c$ .

In conclusion, we have calculated the spin-disorder resistivity of Fe and Ni in the whole temperature range up to  $T_c$  using both the mean-field approximation and the nearest-neighbor Heisenberg model to represent the canonical ensemble of classical spin configurations. We found that SDR is insensitive to the magnetic short-range order (MSRO) in Fe and Ni. The SDR in Fe depends linearly on  $M^2(T)$  which implies that the main effect of spin disorder is to introduce scattering, which is proportional to the variance of the random potential. For Ni the cal-

culated temperature dependence is more complicated; at elevated temperatures close to  $T_c$  the SDR grows faster than expected. This faster increase of SDR may be explained by the reduction of the exchange splitting which lifts the heavy bands up to the Fermi level, thereby increasing the scattering rate. The results for Fe are in very good agreement with experiment if the atomic potentials are taken from zero temperature and frozen, but for Ni the SDR calculated in this way is strongly overestimated. This disagreement is attributed to the reduction of the local magnetic moment in Ni. Comparison with experimental SDR leads to a value of  $0.35\mu_B$  above  $T_c$ , which may be compared with experiment.

### Acknowledgments

We are grateful to V. P. Antropov and E. Y. Tsymbal for useful discussions. This work was supported by the Nebraska Research Initiative, NSF EPSCoR, and NSF MRSEC. K. D. B. is a Cottrell Scholar of Research Corporation. The work was completed utilizing the Research Computing Facility of the University of Nebraska-Lincoln. A portion of this research at Oak Ridge National Laboratory's Center for Nanophase Materials Sciences was sponsored by the Scientific User Facilities Division, Office of Basic Energy Sciences, U.S. Department of Energy.

---

\* Electronic address: awysocki@bigred.unl.edu

<sup>1</sup> B. R. Coles, Adv. Phys. **7**, 40 (1958).

<sup>2</sup> N. F. Mott, Adv. Phys. **13**, 325 (1964).

<sup>3</sup> S. V. Vonsovskii, *Magnetism* (Halsted Press, New York 1974).

<sup>4</sup> R. J. Weiss and A. S. Marotta, J. Phys. Chem. Solids **9**, 302 (1959).

<sup>5</sup> A. Fert and I. A. Campbell, Phys. Rev. Lett. **21**, 1190 (1968); J. Phys. F: Met. Phys. **6**, 849 (1976).

<sup>6</sup> T. Kasuya, Progr. Theor. Phys. **16**, 58 (1956).

<sup>7</sup> P. G. de Gennes and J. Friedel, J. Phys. Chem. Solids **4**, 71 (1958).

<sup>8</sup> I. Mannari, Progr. Theor. Phys. **26**, 51 (1961).

<sup>9</sup> S. V. Vonsovskii and Yu. Izyumov, Sov. Phys. Uspekhi **5**, 547 (1963).

<sup>10</sup> M. E. Fisher and J. S. Langer, Phys. Rev. Lett. **20**, 667 (1968).

<sup>11</sup> J. B. Gibson, J. Phys. Chem. Solids **1**, 27 (1956).

<sup>12</sup> P. L. Rossiter, P. Wells, J. Phys. C: Solid St. Phys. **4**, 354 (1971).

<sup>13</sup> S. Alexander, J. S. Helman, and I. Balberg, Phys. Rev. B **13**, 304 (1976).

<sup>14</sup> M. Kataoka, Phys. Rev. B **63**, 134435 (2001).

<sup>15</sup> K. Akabli and H. T. Diep, J. Appl. Phys. **103**, 07F307 (2008).

<sup>16</sup> D. A. Goodings, Phys. Rev. **132**, 542 (1963).

<sup>17</sup> T. Moriya, *Spin fluctuations in itinerant electron mag-*

*netism* (Springer, Berlin, 1985).

<sup>18</sup> V. P. Antropov, Phys. Rev. B **72**, 140406 (2005).

<sup>19</sup> C. S. Wang, R. E. Prange, and V. Korenman, Phys. Rev. B **25**, 5766 (1982).

<sup>20</sup> A. V. Ruban, S. Khmelevskiy, P. Mohn, and B. Johansson, Phys. Rev. B **75**, 054402 (2007).

<sup>21</sup> A. L. Wysocki, J. K. Glasbrenner, and K. D. Belashchenko, Phys. Rev. B **78**, 184419 (2008).

<sup>22</sup> A. L. Wysocki, K. D. Belashchenko, J. P. Velev and M. van Schilfhaarde, J. Appl. Phys. **101**, 09G506 (2007).

<sup>23</sup> O. K. Andersen, Phys. Rev. B **12**, 3060 (1975).

<sup>24</sup> B. L. Gyorffy, A. J. Pindor, J. Staunton, G. M. Stocks, and H. Winter, J. Phys. F: Met. Phys. **15**, 1337 (1985).

<sup>25</sup> I. Turek, V. Drchal, J. Kudrnovský, M. Šob, and P. Weinberger, *Electronic Structure of Disordered Alloys, Surfaces and Interfaces* (Kluwer, Boston, 1997).

<sup>26</sup> J. Kudrnovský, V. Drchal, C. Blaas, P. Weinberger, I. Turek, and P. Bruno, Phys. Rev. B **62**, 15084 (2000).

<sup>27</sup> S. Datta, *Electronic Transport in Mesoscopic Systems* (Cambridge University Press, Cambridge, 1995).

<sup>28</sup> M. van Schilfhaarde (unpublished).

<sup>29</sup> V. Drchal, J. Kudrnovský, P. Bruno, P. H. Dederichs, I. Turek, and P. Weinberger, Phys. Rev. B **65**, 214414 (2002).

<sup>30</sup> R. H. Brown, P. B. Allen, D. M. Nicholson, and W. H. Butler, Phys. Rev. Lett. **62**, 661 (1989).

<sup>31</sup> I. Turek, J. Kudrnovský, V. Drchal, L. Szunyogh, and P. Weinberger, Phys. Rev. B **65**, 125101 (2002).

- <sup>32</sup> J. Banhart, H. Ebert, P. Weinberger, and J. Voitländer, Phys. Rev. B **50**, 2104 (1994).
- <sup>33</sup> Á. Buruzs, L. Szunyogh, and P. Weinberger, Phil. Mag. **88**, 2615 (2008).
- <sup>34</sup> J. B. Staunton and B. L. Gyorffy, Phys. Rev. Lett. **69**, 371 (1992).
- <sup>35</sup> J. Staunton, B. L. Gyorffy, A. J. Pindor, G. M. Stocks, and H. Winter, J. Phys. F: Met. Phys. **15**, 1387 (1985).
- <sup>36</sup> H. A. Mook, J. W. Lynch, and R. M. Nicklow, Phys. Rev. Lett. **30**, 556 (1973).
- <sup>37</sup> J. Crangle and G. M. Goodman, Proc. R. Soc. London, Ser. A **321**, 477 (1971).
- <sup>38</sup> The MFA criterion of validity is  $1/z \ll 1$  where  $z$  is the effective number of neighbors inside the interaction range.
- <sup>39</sup> V. P. Antropov, B. N. Harmon, and A. N. Smirnov, J. Magn. Magn. Mater. **200**, 148 (1999).
- <sup>40</sup> R. L. McGreevy, J. Phys.: Condens. Matter **13**, R877 (2001).
- <sup>41</sup> V. L. Moruzzi, *et. al.*, Phys. Rev. B **34**, 1784 (1986).